

Estimating mean profiles and fluxes in high-speed turbulent boundary layers using inner/outer-layer transformations

Asif Manzoor Hasan*

Delft University of Technology, Leeghwaterstraat 39, 2628 CB, Delft, The Netherlands

Johan Larsson†

University of Maryland, College Park, MD 20742, USA

Sergio Pirozzoli‡

Sapienza Università di Roma, Via Eudossiana 18, 00184 Roma, Italy

Rene Pecnik§

Delft University of Technology, Leeghwaterstraat 39, 2628 CB, Delft, The Netherlands

Nomenclature

τ_w	= wall shear stress	Re_τ	= $\rho_w u_\tau \delta / \mu_w$, friction Reynolds number
ρ	= density	Re_τ^*	= $\bar{\rho} u_\tau^* \delta / \bar{\mu}$, semi-local friction Reynolds number
μ	= dynamic viscosity	M_τ	= $u_\tau / \sqrt{\gamma RT_w}$, friction Mach number
k	= thermal conductivity	M_∞	= $u_\infty / \sqrt{\gamma RT_\infty}$, free-stream Mach number
c_p	= specific heat capacity at constant pressure	r	= recovery factor
γ	= specific heat capacity ratio	c_f	= $2\tau_w / (\rho_\infty u_\infty^2)$, skin-friction coefficient
T	= temperature	c_h	= $q_w / (c_p \rho_\infty u_\infty (T_w - T_r))$, heat-transfer coefficient
R	= specific gas constant	q_w	= wall heat flux
u_τ	= $\sqrt{\tau_w / \rho_w}$, friction velocity	y	= wall-normal coordinate
u_τ^*	= $\sqrt{\tau_w / \bar{\rho}}$, semi-local friction velocity	y^*	= y / δ_v^* , semi-local wall-normal coordinate
δ_v	= $\mu_w / (\rho_w u_\tau)$, viscous length scale	Pr	= $\mu c_p / k$, Prandtl number
δ_v^*	= $\bar{\mu} / (\bar{\rho} u_\tau^*)$, semi-local viscous length scale	κ	= von Kármán constant
δ	= (or δ_{99}), boundary layer thickness	Π	= Coles' wake parameter
θ	= momentum thickness	C	= log-law intercept
δ^*	= displacement thickness	μ_t	= eddy viscosity
U	= transformed (incompressible) velocity		
u	= untransformed velocity		
Re_θ	= $\rho_\infty u_\infty \theta / \mu_\infty$, momentum thickness Reynolds number		
Re_{δ^*}	= $\rho_\infty u_\infty \delta^* / \mu_\infty$, displacement thickness Reynolds number		
Re_{δ_2}	= $\rho_\infty u_\infty \theta / \mu_w$		
Subscripts			
w	= wall	∞	= free-stream
e	= boundary layer edge ($y = \delta$)	r	= recovery
Superscripts			
$+$	= wall-scaled	$\overline{(\cdot)}$	= Reynolds averaging

*Ph.D. Candidate, Process and Energy Department

†Professor, Department of Mechanical Engineering, Associate Fellow AIAA.

‡Professor, Dipartimento di Ingegneria Meccanica e Aerospaziale

§Professor, Process and Energy Department

I. Introduction

Accurately predicting drag and heat transfer for compressible high-speed flows is of utmost importance for a range of engineering applications. This requires the precise knowledge of the entire velocity and temperature profiles. A common approach is to use compressible velocity scaling laws (transformation), that inverse transform the velocity profile of an incompressible flow, together with a temperature-velocity relation. Current methods [1, 2] typically assume a single velocity scaling law, neglecting the different scaling characteristics of the inner and outer layers. In this Note, we use distinct velocity transformations for these two regions. In the inner layer, we utilize a recently proposed scaling law that appropriately incorporates variable property and intrinsic compressibility effects [3], while the outer layer profile is inverse-transformed with the well-known Van Driest transformation [4]. The result is an analytical expression for the mean shear valid in the entire boundary layer, which combined with the temperature-velocity relationship in Zhang et al. [5], provides predictions of mean velocity and temperature profiles at unprecedented accuracy. Using these profiles, drag and heat transfer is evaluated with an accuracy of $\pm 4\%$ and $\pm 8\%$, respectively, for a wide range of compressible turbulent boundary layers up to Mach numbers of 14.

II. Proposed method

An incompressible velocity profile is composed of two parts: (1) the law of the wall in the inner layer, and (2) the velocity defect law in the outer layer. We can model the law of the wall either by composite velocity profiles [6–8], or by integrating the mean momentum equation using a suitable eddy viscosity model [9, 10]. Here, we follow the latter approach and utilize the Johnson-King [10] eddy viscosity model. Likewise, there are several formulations available to represent the defect law [11–13], of which we use Coles' law of the wake [11].

Once the reference incompressible velocity profile is obtained, we inverse transform it using our recently proposed velocity transformation [3] for the inner layer, and the Van Driest (VD) transformation [4] for the outer layer. They are combined as follows:

$$d\bar{u}^+ = f_3^{-1} f_2^{-1} f_1^{-1} d\bar{U}_{inner}^+ + f_1^{-1} d\bar{U}_{wake}^+, \quad (1)$$

where the factors f_1 , f_2 , and f_3 constitute the transformation kernel proposed in Hasan et al. [3] that accounts for both variable property and intrinsic compressibility effects, given as

$$\frac{d\bar{U}^+}{d\bar{u}^+} = \underbrace{\left(\frac{1 + \kappa y^* D(M_\tau)}{1 + \kappa y^* D(0)} \right)}_{f_3} \underbrace{\left(1 - \frac{y}{\delta_v^*} \frac{d\delta_v^*}{dy} \right)}_{f_2} \underbrace{\sqrt{\frac{\bar{\rho}}{\rho_w}}}_{f_1}, \quad (2)$$

where

$$D(M_\tau) = \left[1 - \exp\left(\frac{-y^*}{A^+ + f(M_\tau)} \right) \right]^2. \quad (3)$$

The value of A^+ differs based on the choice of the von Kármán constant κ , such that the log-law intercept is reproduced for that κ [8]. With $\kappa = 0.41$, the value of $A^+ = 17$ gives a log-law intercept of 5.2 [14], whereas, with $\kappa = 0.384$, $A^+ = 15.22$ gives a log-law intercept of 4.17. The additive term $f(M_\tau)$ accounts for intrinsic compressibility effects. Hasan et al. [3] proposed $f(M_\tau) = 19.3M_\tau$, that is independent of the chosen value of κ . In Eq. (1), $d\bar{U}_{inner}^+$ is modeled using the Johnson-King eddy viscosity model as $dy^*/[1 + \kappa y^* D(0)]$, which after integration, recovers the incompressible law of the wall, and $d\bar{U}_{wake}^+ = \Pi/\kappa \sin(\pi y/\delta) \pi d(y/\delta)$ is the derivative of the Coles' wake function [7].

Inserting the expressions for $d\bar{U}_{inner}^+$, $d\bar{U}_{wake}^+$ in Eq. (1), using $dy^*/dy = f_2/\delta_v^*$, $u_\tau^* = u_\tau f_1^{-1}$, and upon rearrangement, we get the dimensional form of the mean velocity gradient as

$$\frac{d\bar{u}}{dy} = \frac{u_\tau^*}{\delta_v^*} \frac{1}{1 + \kappa y^* D(M_\tau)} + \frac{u_\tau^*}{\delta} \frac{\Pi}{\kappa} \pi \sin\left(\pi \frac{y}{\delta}\right). \quad (4)$$

Eq. (4) provides several useful insights. Analogous to an incompressible flow, the mean velocity in a compressible flow is controlled by two distinct length scales, δ_v^* and δ , characteristic of the inner and outer layers, respectively. The two layers are connected by a common velocity scale u_τ^* (the semi-local friction velocity), leading to a logarithmic law in the overlap region between them. Moreover, in the overlap layer, the denominator of the first term on the right-hand side reduces to κy , consistent with Townsend's attached-eddy hypothesis. The second term on the right-hand-side is the wake term accounting for mean density variations, where Coles' wake parameter Π depends on the Reynolds number, as discussed in the subsection below.

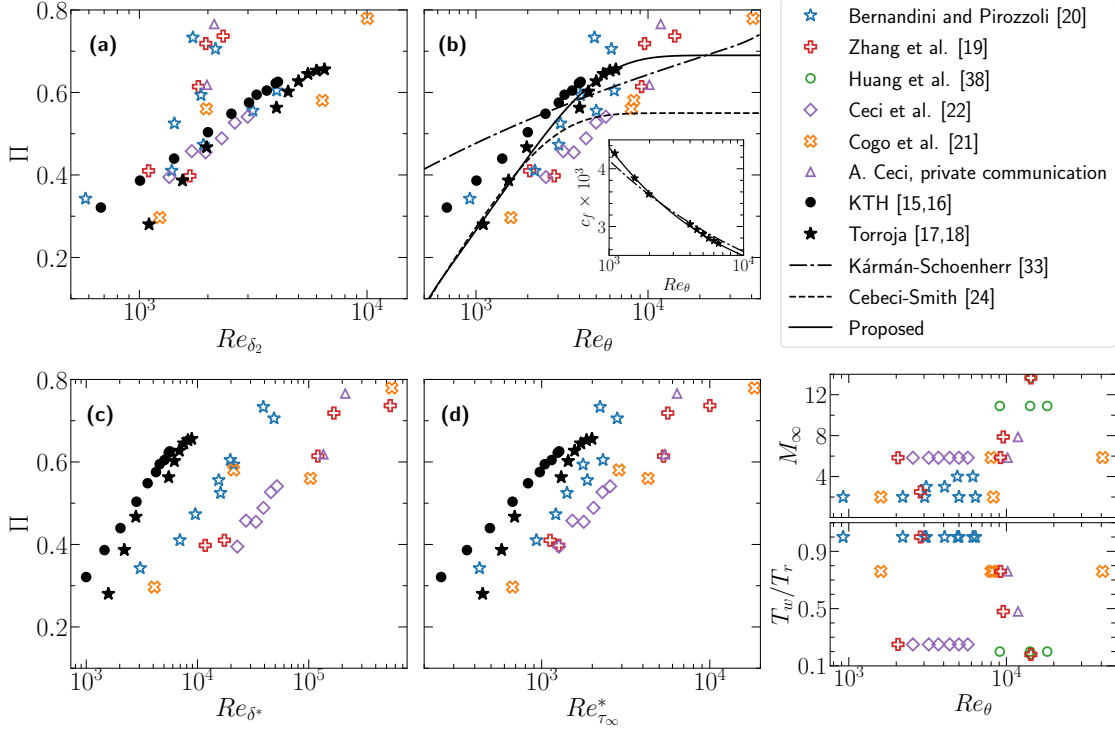


Fig. 1 The wake parameter Π computed using the DNS data and plotted as a function of (a) Re_{δ_2} (b) Re_{θ} (c) Re_{δ^*} and (d) $Re_{\tau_{\infty}^*}$ for 19 incompressible [15–18] and 26 compressible [19–22, A. Ceci, private communication] turbulent boundary layers.

A. Characterizing low-Reynolds-number effects on the wake parameter

For incompressible boundary layers, Coles’ wake parameter is known to strongly depend on Re_{θ} at low Reynolds numbers [13, 23, 24]. For compressible boundary layers, the ambiguity of the optimal Reynolds number definition poses a challenge to characterize the wake parameter. Fernholz and Finley [25], mainly using experimental data at that time, observed that the momentum-thickness Reynolds number with viscosity at the wall (Re_{δ_2}) is the suitable definition to scale Π . However, intuitively, Π should scale with Reynolds number based on the free-stream properties [24, 26]. Given the recent availability of Direct Numerical Simulation (DNS) data at moderate Reynolds numbers for both compressible and incompressible flows, we revisit the question of which Reynolds number best describes the wake parameter.

First, we evaluate Π for several incompressible and compressible DNS cases from the literature and then report it as a function of different definitions of the Reynolds number, searching for the definition yielding the least spread of the data points. For incompressible flows, the wake strength can be determined as $\Pi = 0.5\kappa (\bar{U}^+(y = \delta) - 1/\kappa \ln(\delta^+) - C)$, where C is the log-law intercept for the chosen κ . For compressible flows, the wake strength is based on the VD transformed velocity [25, 26] as $\Pi = 0.5\kappa (\bar{U}_{vd}^+(y = \delta) - (\bar{U}_{vd}^+)^{log}(y = \delta))$, where \bar{U}_{vd}^+ is obtained from the DNS data. The reference log law $(\bar{U}_{vd}^+)^{log}$, unlike for incompressible flows, cannot be computed as $1/\kappa \ln(y^+) + C_{vd}$, because C_{vd} is found to be non-universal for diabatic compressible boundary layers [27, 28]. Hence, $(\bar{U}_{vd}^+)^{log}$ can be obtained either by fitting a logarithmic curve to \bar{U}_{vd}^+ [25], or by inverse transforming the incompressible law of the wall. Here, we follow the latter approach by using the compressibility transformation of Hasan et al. [3].

The value of the von Kármán constant κ plays a crucial role in estimating Π . Spalart [29] noted that a strong consensus on κ is needed to accurately estimate Π . However, such a consensus is yet missing [30]. Recently, Nagib and Chauhan [8] showed that $\kappa = 0.384$ is a suitable choice for incompressible boundary layers, verified to be true also for channels [31] and pipes [32]. However, due to historical reasons and wide acceptance of $\kappa = 0.41$, we will proceed with this value. The same procedure can straightforwardly be repeated with a different value of κ .

Figure 1 shows the wake parameter for twenty-six compressible and nineteen incompressible boundary layer flows, as a function of Re_{δ_2} , Re_{θ} , Re_{δ^*} and $Re_{\tau_{\infty}^*}$. The spread in the data points is found to be quite large for all the definitions, as Π is the difference of two relatively large quantities, namely \bar{U}_{vd}^+ and $(\bar{U}_{vd}^+)^{log}$ at the boundary layer edge, as

outlined above. Note that even incompressible boundary layers are not devoid of this scatter [13, 29]. Figure 1(a) shows the presence of two distinct branches, hence Re_{δ_2} does not seem to be suitable to characterize Π , unlike reported in previous literature [1, 25]. Among the four definitions of Reynolds number, Re_θ seems to show the least spread. Figure 1(b) also reports several functional forms of $\Pi = f(Re_\theta)$. Use of the modified Kármán-Schoenherr friction formula [33] for indirect evaluation of Π , does not show saturation at high Reynolds numbers as observed in Coles [23] for incompressible flows. The Cebeci-Smith relation [24] underpredicts Π , but reproduces saturation at high Reynolds numbers. We thus propose a relation similar to that proposed by [24], with modified constants to achieve a better fit with data from recent incompressible DNS [17, 18]. The relation is

$$\Pi = 0.69 \left[1 - \exp(-0.243\sqrt{z} - 0.15z) \right], \quad \text{where } z = Re_\theta/425 - 1. \quad (5)$$

Inset in Fig. 1(b) compares the skin-friction curve computed using Eq. (5) with the modified Kármán-Schoenherr skin-friction formula [33]. The distance between the two curves is large at low Reynolds numbers, but less so at higher Reynolds numbers. As expected, the incompressible DNS data of Jiménez et al. [17], Sillero et al. [18], follow the friction curve computed using Eq. (5).

B. Implementation of the proposed method

For convenience, Eq. (4) can also be expressed in terms of the dimensional variables τ_w , $\bar{\mu}$ and $\bar{\rho}$ as,

$$\frac{d\bar{u}}{dy} = \frac{\tau_w}{\bar{\mu} + \underbrace{\sqrt{\tau_w \bar{\rho}} \kappa y D(M_\tau)}_{\mu_t}} + \frac{\sqrt{\tau_w/\bar{\rho}}}{\delta} \frac{\Pi}{\kappa} \pi \sin\left(\pi \frac{y}{\delta}\right), \quad (6)$$

where μ_t is the Johnson-King eddy viscosity model corrected for intrinsic compressibility effects, derived from Hasan et al. [3] transformation. It can be readily used in turbulence modeling, for instance, as a wall-model in Large Eddy Simulations. Note that different eddy viscosity models can be used in Eq. (6), for example, Prandtl's mixing length model (see Appendix A). Eq. (6) covers the entire boundary layer, and it can be integrated in conjunction with a suitable temperature model such as the one proposed by Zhang et al. [5], which is given as

$$\frac{\bar{T}}{T_w} = 1 + \frac{T_r - T_w}{T_w} \left[(1 - sPr) \left(\frac{\bar{u}}{u_\infty} \right)^2 + sPr \left(\frac{\bar{u}}{u_\infty} \right) \right] + \frac{T_\infty - T_r}{T_w} \left(\frac{\bar{u}}{u_\infty} \right)^2, \quad (7)$$

where $sPr = 0.8$, $T_r/T_\infty = 1 + 0.5r(\gamma - 1)M_\infty^2$, and $r = Pr^{1/3}$. Moreover, a suitable viscosity law (e.g., power or Sutherland's law), and the ideal gas equation of state $\bar{\rho}/\rho_w = T_w/\bar{T}$ have to be used to compute mean viscosity and density profiles, respectively. The inputs that need to be provided are the Reynolds number (Re_θ), free-stream Mach number (M_∞), wall cooling/heating parameter (T_w/T_r) and (optionally) the dimensional wall or free-stream temperature for Sutherland's law. It is important to note that Eq. (7), and all solver inputs are based on the quantities in the free-stream, and not at the boundary layer edge. For more insights on the solver, please refer to the source code available on GitHub [34].

III. Results

Figure 2 shows the predicted velocity and temperature profiles for a selection of high Mach number cases. As can be seen, the DNS and the predicted profiles are in good agreement, thus corroborating our methodology. The insets in Figure 2 show the error in the predicted skin-friction and heat-transfer coefficients for thirty compressible cases from the literature. For most cases, the friction coefficient (c_f) is predicted with $\pm 4\%$ accuracy, with a maximum error of -5.3% . The prediction of the heat-transfer coefficient (c_h) shows a slightly larger error compared to c_f , potentially due to additional inaccuracies arising from the temperature-velocity relation. In most cases, c_h is predicted with $\pm 8\%$ accuracy, with a maximum error of 10.3% .

The proposed method is modular in that it can also be applied using other inner-layer transformations [28, 35, 36] with minor modifications as discussed in Appendix B. This is shown in Figure 3, which compares the proposed approach with another modular approach of Kumar and Larsson [2], both with different inner layer transformations. Additionally, the figure includes results obtained with the method of Huang et al. [1] using the VD transformation, and the widely recognized Van Driest II skin-friction formula [37]. Figure 3 also shows the root-mean-square error, determined as

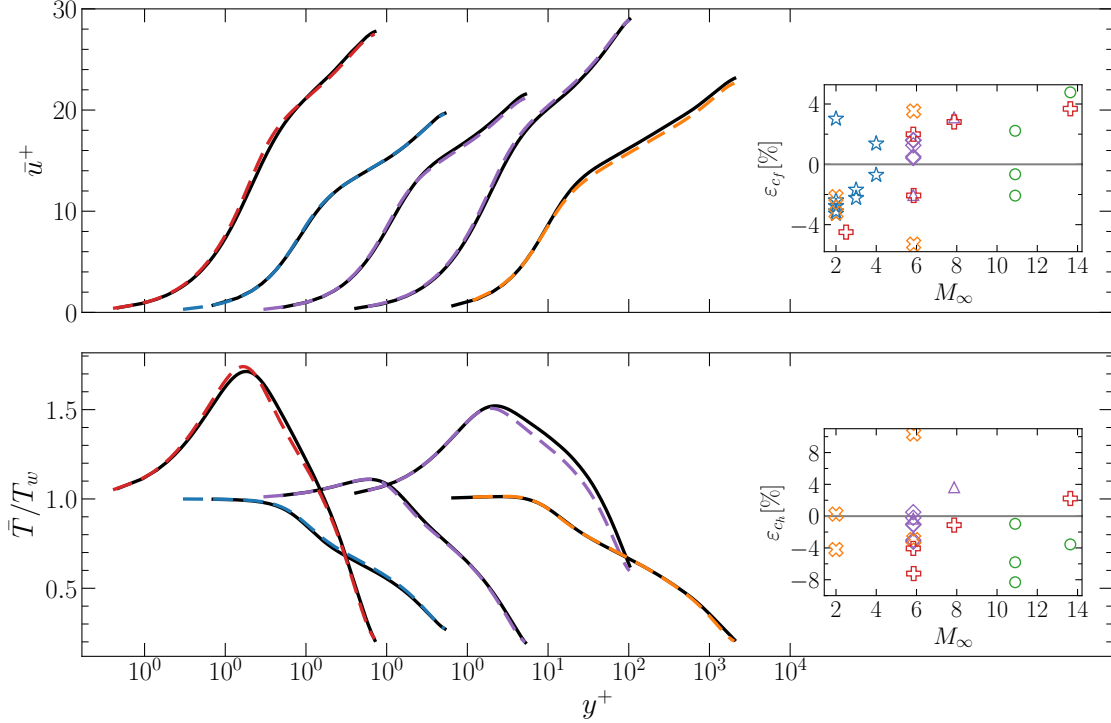


Fig. 2 Predicted velocity (top) and temperature (bottom) profiles (dashed lines) compared to DNS (black solid lines) for the cases with the highest reported Mach numbers in the respective publications: (left to right) $M_\infty = 13.64$, $T_w/T_r = 0.18$ [19]; $M_\infty = 4$, $T_w/T_r = 1$ [20]; $M_\infty = 7.87$, $T_w/T_r = 0.48$ (A. Ceci, private communication); $M_\infty = 5.84$, $T_w/T_r = 0.25$ [22]; $M_\infty = 5.86$, $T_w/T_r = 0.76$ [21]. (Insets): Percent error in skin-friction (top) and heat-transfer (bottom) prediction for 30 compressible turbulent boundary layers from the literature [19–22, 38, A. Ceci, private communication]. The error is computed as $\varepsilon_{c_f} = (c_f - c_f^{DNS})/c_f^{DNS} \times 100$ and likewise for ε_{c_h} . Symbols are as in Figure 1.

$RMS = \sqrt{1/N \sum \varepsilon_{c_f}^2}$, where N is the total number of DNS cases considered. The Van Driest II formula and the method of Huang et al. have similar RMS error of about 6%*, which is not surprising as both of them are built on Van Driest’s mixing-length arguments. The errors are selectively positive for majority of the cases, and it increases with higher Mach number and stronger wall cooling. The source of this error mainly resides in the inaccuracy of the VD velocity transformation in the near-wall region for diabatic flows. To eliminate this shortcoming, Kumar and Larsson [2] developed a modular methodology, which is quite accurate when the transformation of Volpiani et al. [36] is used, but it is less accurate if other velocity transformations are implemented. This inaccuracy is because the outer layer velocity profile is also inverse-transformed according to the inner-layer transformation. In the current approach, the velocity profile is instead inverse-transformed using two distinct transformations, which take into account the different scaling properties of the inner and outer layers, thus reducing the RMS error with respect to Kumar and Larsson’s modular method for all the transformations tested herein. The error using the proposed approach with the TL transformation is preferentially positive for all the cases. This is due to the log-law shift observed in the TL scaling, which is effectively removed in the Hasan et al. transformation, thereby yielding an RMS error of 2.66%, which is the lowest among all approaches.

IV. Conclusions

We have derived an expression for the mean velocity gradient in high-speed boundary layers [Eq. (6)] that combines the inner-layer transformation recently proposed by Hasan et al. [3] and the Van Driest [4] outer-layer transformation, thus covering the entire boundary layer. The Coles’ wake parameter in this expression is determined using an

*Huang et al.’s method with the more accurate temperature velocity relation in Zhang et al. [5] leads to an RMS error of 12%.

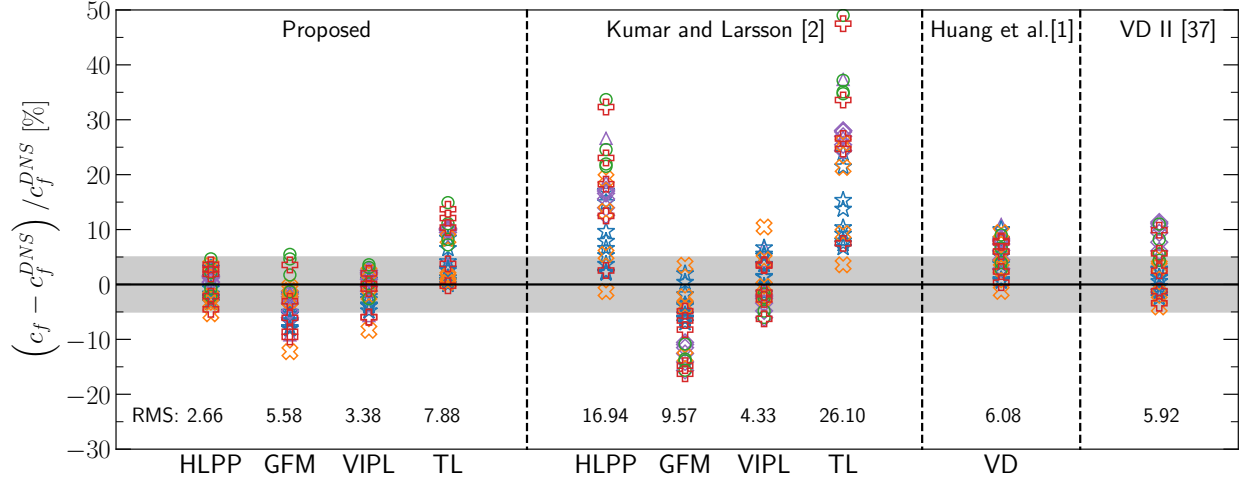


Fig. 3 Error in skin-friction prediction using the proposed approach compared to different state-of-the-art approaches. The letters on the X-axis denote the velocity transformation used for that approach. HLPP, GFM, VIPL, TL, and VD stand for the transformations proposed in Hasan et al. [3], Griffin et al. [35], Volpiani et al. [36], Trettel and Larsson [28], and Van Driest [4], respectively. The numbers are RMS values computed as outlined in the text. Symbols are as in Figure 1. The shaded region shows an error bar of +/-5%. Note that inputs for all the methods are based on properties in the free-stream instead of at the edge of the boundary layer.

adjusted Cebeci and Smith relation [Eq. (5)] with the definition of Re_θ as the most suitable parameter to characterize low-Reynolds-number effects on Π . This method allows remarkably accurate predictions of the mean velocity and temperature profiles, leading to estimation of the friction and heat-transfer coefficients which are within +/-4% and +/-8% error bounds with respect to DNS data, respectively.

The skin-friction results are compared with that from other state-of-the-art approaches considered in literature. Limited accuracy of the VD II and Huang et al.'s methods is attributable to inaccuracy of the underlying VD transformation in the near-wall region of diabatic boundary layers, whereas inaccuracy in Kumar and Larsson's approach is attributable to the unsuitability of the inner layer velocity transformations in the outer layer. By combining different scaling laws in the inner layer with the Van Driest transformation in the outer layer, our method demonstrates improved results for all the inner-layer transformations herein tested, with the lowest RMS error of 2.66% achieved with Hasan et al.'s transformation.

The methodology developed in this note promises straightforward application to other classes of wall-bounded flows like channels and pipes, upon change of the temperature-velocity relation [e.g. 39], and using different values of the wake parameter Π [8]. Also, the method is modular in the sense that it can be used with other temperature models and equations of state.

Acknowledgements

We thank Dr. P. Costa for the insightful discussions. This work was supported by the European Research Council grant no. ERC-2019-CoG-864660, Critical; and the Air Force Office of Scientific Research under grants FA9550-19-1-0210 and FA9550-19-1-7029.

Appendix A: Mean shear using Prandtl's mixing length model

The choice of the eddy viscosity model affects the first term on the right hand side of Eq. (6). By analogy, the mean shear equation using Prandtl's mixing length model is thus as follows,

$$\frac{d\bar{u}}{dy} = \frac{2\tau_w}{\bar{\mu} + \sqrt{\bar{\mu}^2 + [2\sqrt{\tau_w}\bar{\rho}\kappa y D(M_\tau)]^2}} + \frac{\sqrt{\tau_w/\bar{\rho}}}{\delta} \frac{\Pi}{\kappa} \pi \sin\left(\pi \frac{y}{\delta}\right), \quad (8)$$

where $D(M_\tau)$ is the damping function corrected for intrinsic compressibility effects as

$$D(M_\tau) = 1 - \exp\left(\frac{-y^*}{A^+ + 39M_\tau}\right), \quad (9)$$

with $A^+ = 25.53$ (or 26) for $\kappa = 0.41$, and where the additive term $39M_\tau$ is obtained following similar steps as for the Johnson-King model (see Ref. [3]).

Appendix B: Implementation of the method using velocity transformations in Ref. [35, 36]

In the logarithmic region and beyond, the first term on the right-hand side of Eq. (6) reduces to $\sqrt{\tau_w/\bar{\rho}}/(\kappa y)$, which is the same as Van Driest's original arguments [4]. It is crucial to satisfy this condition, otherwise the logarithmic profile extending to the outer layer would not obey Van Driest's scaling. The transformations of Griffin et al. [35], Volpiani et al. [36] fail to satisfy this property. To address this issue, we enforce Van Driest's scaling in the outer layer by modifying Eq. (1) as follows

$$\begin{aligned} y_T^+ \leq 50 : \quad d\bar{u}^+ &= \mathcal{T}^{-1} d\bar{U}_{inner}^+ + f_1^{-1} d\bar{U}_{wake}^+, \\ y_T^+ > 50 : \quad d\bar{u}^+ &= f_1^{-1} d\bar{U}_{inner}^+ + f_1^{-1} d\bar{U}_{wake}^+, \end{aligned} \quad (10)$$

where \mathcal{T} denotes the inner-layer transformation kernel and y_T^+ is the transformed coordinate. The value of 50 is taken arbitrarily as a start of the logarithmic region.

References

- [1] Huang, P., Bradshaw, P., and Coakley, T., "Skin friction and velocity profile family for compressible turbulent boundary layers," *AIAA journal*, Vol. 31, No. 9, 1993, pp. 1600–1604.
- [2] Kumar, V., and Larsson, J., "Modular Method for Estimation of Velocity and Temperature Profiles in High-Speed Boundary Layers," *AIAA Journal*, Vol. 60, No. 9, 2022, pp. 5165–5172.
- [3] Hasan, A. M., Larsson, J., Pirozzoli, S., and Pecnik, R., "Incorporating intrinsic compressibility effects in velocity transformations for wall-bounded turbulent flows," , 2023.
- [4] Van Driest, E. R., "Turbulent boundary layer in compressible fluids," *Journal of the Aeronautical Sciences*, Vol. 18, No. 3, 1951, pp. 145–160.
- [5] Zhang, Y.-S., Bi, W.-T., Hussain, F., and She, Z.-S., "A generalized Reynolds analogy for compressible wall-bounded turbulent flows," *Journal of Fluid Mechanics*, Vol. 739, 2014, pp. 392–420.
- [6] Musker, A., "Explicit expression for the smooth wall velocity distribution in a turbulent boundary layer," *AIAA Journal*, Vol. 17, No. 6, 1979, pp. 655–657.
- [7] Chauhan, K., Nagib, H., and Monkewitz, P., "On the composite logarithmic profile in zero pressure gradient turbulent boundary layers," *45th AIAA Aerospace Sciences Meeting and Exhibit*, 2007, p. 532.
- [8] Nagib, H. M., and Chauhan, K. A., "Variations of von Kármán coefficient in canonical flows," *Physics of fluids*, Vol. 20, No. 10, 2008, p. 101518.
- [9] Van Driest, E. R., "On turbulent flow near a wall," *Journal of the aeronautical sciences*, Vol. 23, No. 11, 1956, pp. 1007–1011.
- [10] Johnson, D. A., and King, L., "A mathematically simple turbulence closure model for attached and separated turbulent boundary layers," *AIAA journal*, Vol. 23, No. 11, 1985, pp. 1684–1692.
- [11] Coles, D., "The law of the wake in the turbulent boundary layer," *Journal of Fluid Mechanics*, Vol. 1, No. 2, 1956, pp. 191–226.
- [12] Zagarola, M. V., and Smits, A. J., "A new mean velocity scaling for turbulent boundary layers," *Proceedings of FEDSM*, Vol. 98, 1998, pp. 21–25.
- [13] Fernholz, H., and Finley, P., "The incompressible zero-pressure-gradient turbulent boundary layer: an assessment of the data," *Progress in Aerospace Sciences*, Vol. 32, No. 4, 1996, pp. 245–311.

- [14] Iyer, P. S., and Malik, M. R., “Analysis of the equilibrium wall model for high-speed turbulent flows,” *Physical Review Fluids*, Vol. 4, No. 7, 2019, p. 074604.
- [15] Schlatter, P., Örlü, R., Li, Q., Brethouwer, G., Fransson, J. H., Johansson, A. V., Alfredsson, P. H., and Henningson, D. S., “Turbulent boundary layers up to $Re_{\theta} = 2500$ studied through simulation and experiment,” *Physics of fluids*, Vol. 21, No. 5, 2009, p. 051702.
- [16] Schlatter, P., and Örlü, R., “Assessment of direct numerical simulation data of turbulent boundary layers,” *Journal of Fluid Mechanics*, Vol. 659, 2010, pp. 116–126.
- [17] Jiménez, J., Hoyas, S., Simens, M. P., and Mizuno, Y., “Turbulent boundary layers and channels at moderate Reynolds numbers,” *Journal of Fluid Mechanics*, Vol. 657, 2010, pp. 335–360.
- [18] Sillero, J. A., Jiménez, J., and Moser, R. D., “One-point statistics for turbulent wall-bounded flows at Reynolds numbers up to $\delta^+ = 2000$,” *Physics of Fluids*, Vol. 25, No. 10, 2013, p. 105102.
- [19] Zhang, C., Duan, L., and Choudhari, M. M., “Direct numerical simulation database for supersonic and hypersonic turbulent boundary layers,” *AIAA Journal*, Vol. 56, No. 11, 2018, pp. 4297–4311.
- [20] Bernardini, M., and Pirozzoli, S., “Wall pressure fluctuations beneath supersonic turbulent boundary layers,” *Physics of Fluids*, Vol. 23, No. 8, 2011, p. 085102.
- [21] Cogo, M., Salvatore, F., Picano, F., and Bernardini, M., “Direct numerical simulation of supersonic and hypersonic turbulent boundary layers at moderate-high Reynolds numbers and isothermal wall condition,” *Journal of Fluid Mechanics*, Vol. 945, 2022, p. A30.
- [22] Ceci, A., Palumbo, A., Larsson, J., and Pirozzoli, S., “Numerical tripping of high-speed turbulent boundary layers,” *Theoretical and Computational Fluid Dynamics*, Vol. 36, No. 6, 2022, pp. 865–886.
- [23] Coles, D., “The turbulent boundary layer in a compressible fluid. RAND Corp., Rep,” Tech. rep., R-403-PR, 1962.
- [24] Cebeci, T., and Smith, A. M. O., *Analysis of turbulent boundary layers*, Elsevier, 1974.
- [25] Fernholz, H.-H., and Finley, P., “A critical commentary on mean flow data for two-dimensional compressible turbulent boundary layers,” Tech. rep., AGARD-AG-253, 1980.
- [26] Smits, A. J., and Dussauge, J.-P., *Turbulent shear layers in supersonic flow*, Springer Science & Business Media, 2006.
- [27] Bradshaw, P., “Compressible turbulent shear layers,” *Annual Review of Fluid Mechanics*, Vol. 9, No. 1, 1977, pp. 33–52.
- [28] Trettel, A., and Larsson, J., “Mean velocity scaling for compressible wall turbulence with heat transfer,” *Physics of Fluids*, Vol. 28, No. 2, 2016, p. 026102.
- [29] Spalart, P. R., “Direct simulation of a turbulent boundary layer up to $Re_{\theta} = 1410$,” *Journal of fluid mechanics*, Vol. 187, 1988, pp. 61–98.
- [30] Monkewitz, P. A., and Nagib, H. M., “The hunt for the Kármán “constant” revisited,” , 2023.
- [31] Lee, M., and Moser, R. D., “Direct numerical simulation of turbulent channel flow up to,” *Journal of fluid mechanics*, Vol. 774, 2015, pp. 395–415.
- [32] Pirozzoli, S., Romero, J., Fatica, M., Verzicco, R., and Orlandi, P., “One-point statistics for turbulent pipe flow up to,” *Journal of fluid mechanics*, Vol. 926, 2021.
- [33] Nagib, H. M., Chauhan, K. A., and Monkewitz, P. A., “Approach to an asymptotic state for zero pressure gradient turbulent boundary layers,” *Philosophical Transactions of the Royal Society A: Mathematical, Physical and Engineering Sciences*, Vol. 365, No. 1852, 2007, pp. 755–770.
- [34] Pecnik, R., and Hasan, A. M., “A jupyter notebook to estimate mean profiles and fluxes for high-speed boundary layers,” , 2023. URL <https://github.com/Fluid-Dynamics-Of-Energy-Systems-Team/DragandHeatTransferEstimation.git>.
- [35] Griffin, K. P., Fu, L., and Moin, P., “Velocity transformation for compressible wall-bounded turbulent flows with and without heat transfer,” *Proceedings of the National Academy of Sciences*, Vol. 118, No. 34, 2021, p. e2111144118.
- [36] Volpiani, P. S., Iyer, P. S., Pirozzoli, S., and Larsson, J., “Data-driven compressibility transformation for turbulent wall layers,” *Physical Review Fluids*, Vol. 5, No. 5, 2020, p. 052602.

- [37] Van Driest, E. R., *The problem of aerodynamic heating*, Institute of the Aeronautical Sciences, 1956.
- [38] Huang, J., Nicholson, G. L., Duan, L., Choudhari, M. M., and Bowersox, R. D., "Simulation and modeling of cold-wall hypersonic turbulent boundary layers on flat plate," *AIAA Scitech 2020 Forum*, 2020, p. 0571.
- [39] Song, Y., Zhang, P., Liu, Y., and Xia, Z., "Central mean temperature scaling in compressible turbulent channel flows with symmetric isothermal boundaries," *Physical Review Fluids*, Vol. 7, No. 4, 2022, p. 044606.